16

Application of Carbon Nanotubes Modified Electrode in Pharmaceutical Analysis

Lingbo Qu[1,2] and Suling Yang[1]
[1]*Department of Chemistry, Zhengzhou University, Zhengzhou 450001,*
[2]*Chemistry and Chemical Engineering School, Henan University of Technology, Zhengzhou 450001,*
PR China

1. Introduction

The development of electrochemical sensors has attracted considerable attention as a low-cost method to the sensitive detection of a variety of pharmaceutical analytes. Since the discovery of carbon nanotubes (CNTs) in 1991 [1], research on CNTs has grown rapidly. In recent years, CNTs have also been used as electrode modified materials because CNTs offer unique advantages including enhanced electronic properties, a large edge plane/basal plane ratio, and electron transfer reactions [2]. Thus, CNTs-based sensors generally have higher sensitivities in a low concentration or in the complex matrix, lower limits of detection, and faster electron transfer kinetics than traditional carbon electrodes. Many factors need to be investigated in order to create an optimal CNTs-based sensor. Electrode performance can be influenced by the pretreatment of the nanotube, CNTs surface modification, the method of electrode attachment, and the addition of electron mediators. With the further development of CNTs and nanotechnology, studies on preparation, properties and application of CNTs-based modified electrodes have still been a hot topic attracting lots of researchers in the world. This article is presented on the application of CNTs modified electrode in different pharmaceutical analytes, which mainly includes the electrochemical studies on weak basic pharmaceuticals, weak acidic pharmaceuticals and other related small biological molecules. The physical and catalytic properties make CNTs ideal for use in sensors. Most notably, CNTs display high electrical conductivity, chemical stability, and mechanical strength.

2. CNTs modified electrode used in analysis of weak basic pharmaceuticals

Caffeine (3, 7-dihydro-1, 3, 7-trimethyl-1H-purine-2, 6-dione) and theophylline (3, 7-dihydro-1, 3-dimethyl-1H-purine-2, 6-dione), are two important active alkaloids that are widely distributed in beverages and plant products mainly including tea, coffee bean, cocoa and cola nuts. They are known to have many pharmacological effects, such as gastric acid secretion, diuretic, cardiac stimulant, and stimulant of central nervous system [3]. However, appropriate dosing is crucial because of the serious side adverse reactions in the presence of high concentrations of these compounds as the risk factors for asthma, kidney malfunction and cardiovascular diseases [4].

Nafion, a perfluorinated sulphonated cation exchanger with properties of excellent antifouling capacity, chemical inertness and high permeability to cations, has been extensively employed as an electrode modifier. CNTs can be homogeneously dispersed in Nafion solution because of the hydrophobic side chains and polar head groups of Nafion. Nafion/CNTs composite thin film-modified electrodes have their attractive effects in electroanalytical applications. Recently, we [5, 6] reported that Nafion/CNTs -modified electrode was made, and used as a sensor in the electrochemical determination of caffeine and theophylline. This sensor can ameliorate the problems of high overpotential, slow electrode reaction, and low sensitivity, which occurs at conventional electrodes.
Figure 1 displays the characterization of the Nafion/CNTs composite film on the glassy carbon electrode (GCE) by using scanning electron microscopy (SEM). It is obvious that the Nafion/CNTs composite film was uniformly coated on the electrode surface and formed a spaghetti-like porous reticular formation. The special surface morphology offered a much larger real surface area than the apparent geometric area.

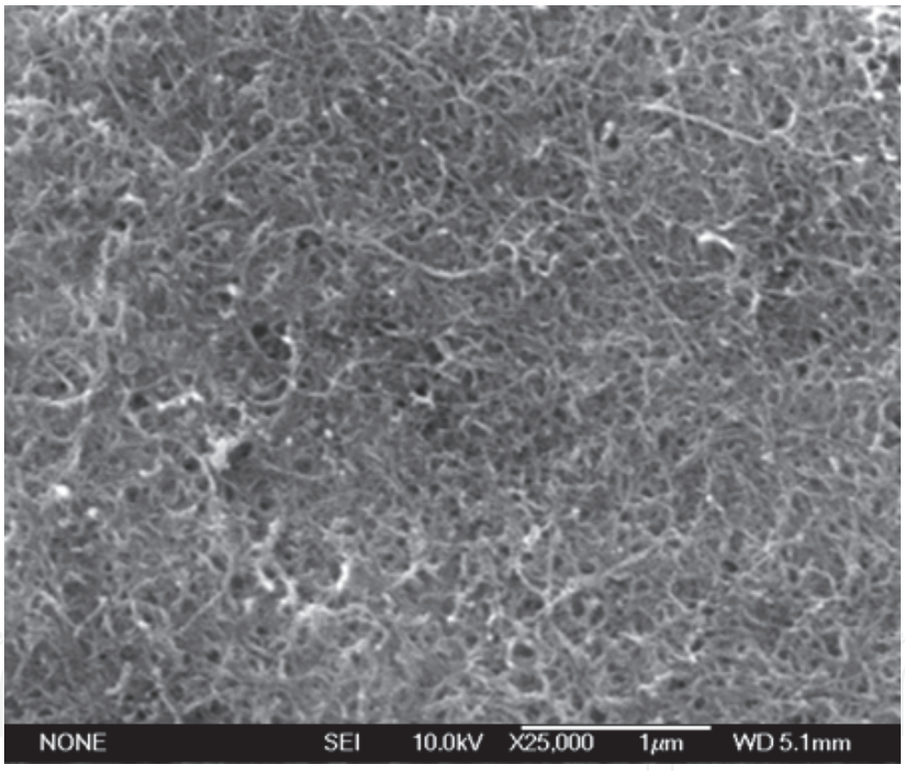

Fig. 1. SEM image of Nafion/CNTs composite film on glassy carbon electrode.

The experimental results demonstrated that caffeine and theophylline can be effectively accumulated at Nafion/CNTs composite film-modified electrode and produce a sensitive anodic peak in a 0.01 mol/L H_2SO_4 medium, respectively (Figure 2). Under the same conditions, no anodic peak of caffeine and theophyline was observed at the bare GCE. Especially at the Nafion/CNTs nanocomposite -modified electrode, the peak current was significantly higher than those at the CNTs/GCE or the Nafion/GCE. The oxidation process of caffeine and theophyline at Nafion/CNTs/GCE or Nafion/GCE is irreversible. Compared with the Nafion/GCE, the oxidation potential at the Nafion/CNTs/GCE was

negatively shifted. This phenomenon may be an evidence of catalytic effect of CNTs toward caffeine and theophyline oxidation. The reasons for the notable sensitivity of the determination at the Nafion/CNTs/GCE may be summarized as follows:(1) the Nafion/CNTs/GCE contains the cation exchanger of Nafion which has selective cation exchange enriched ability due to the electrostatic interaction. (2) CNTs display attractive characteristics, such as much larger specific surface area, excellent adsorptive ability and catalytic ability. Without a doubt, the synergetic functions of Nafion and CNTs make contributions to the higher current response [7-12].

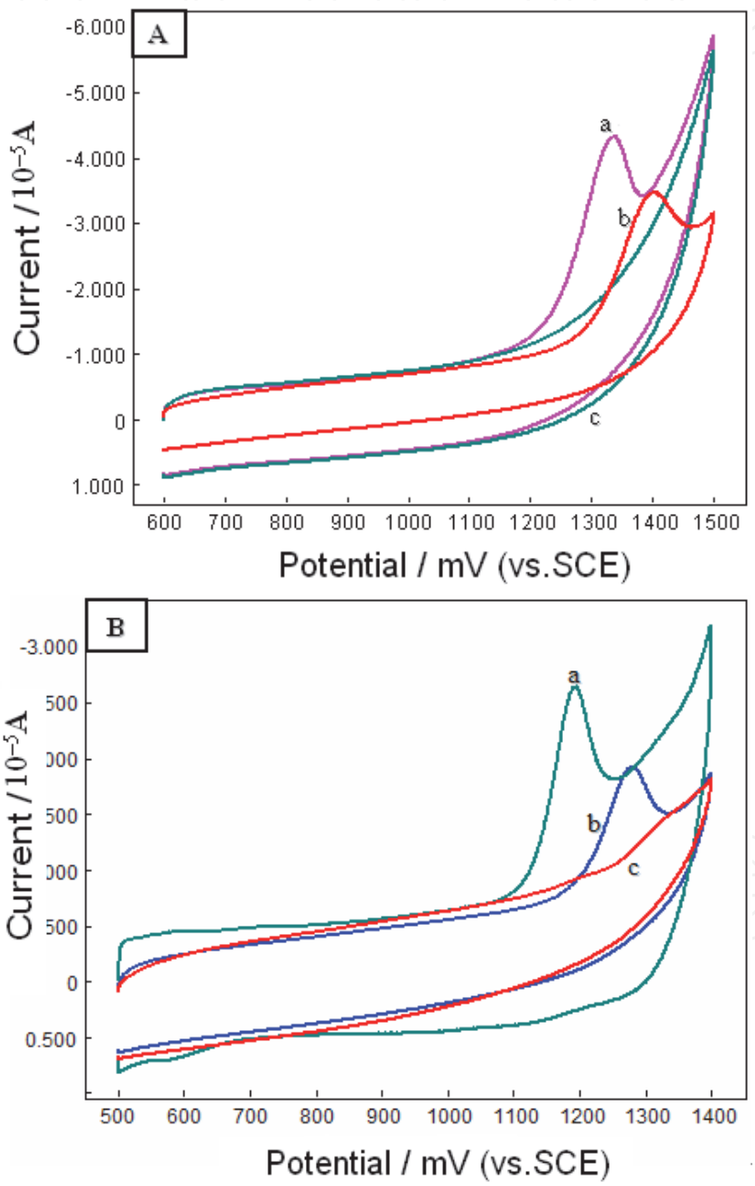

Fig. 2. Cyclic voltammograms of the Nafion/CNTs-modified GCE (a), Nafion-modified GCE (b), the bare GCE (c) in 0.01 mol/L H_2SO_4 medium containing: A. 3.0 ×10^{-5} mol/L caffeine; scan rate 80 mV/s; B. 2.0 × 10^{-5} mol/L theophyline; scan rate 100 mV/s.

Under the suitable conditions, the anodic peak current was linear to caffeine concentration in the range of $6.0 \times 10^{-7} - 4.0 \times 10^{-4}$ mol/L with a limit of detection of 2.3×10^{-7} mol/L; theophylline in the range of $8.0 \times 10^{-8} - 6.0 \times 10^{-5}$ mol/L with a detection limit of 2.0×10^{-8} mol/L.

Regeneration and reproducibility are the two vital characteristics for the modified electrode, which should be investigated for analytical determination. The same Nafion/CNTs/GCE was used for five times successive measurement of 2.0×10^{-5} mol/L TP. After each measurement, the surface of the Nafion/CNTs/GCE was regenerated by successively scan cycle between 500 and 1400 mV in 0.01 mol/L H_2SO_4 medium solutions for three cycles. The relative standard deviation (RSD) of the peak current was 2.4% (n = 5), which revealed the good regeneration and reproducibility.

This newly exploited method was successfully used to determine caffeine in beverage samples and theophylline in drug samples. The detected results of caffeine in beverage samples are shown in Table 1. The results are in agreement with the value obtained employing UV–vis spectroscopic method [13] as well as the regulation of the American Beverage Association [14] in the range of $4.3 \times 10^{-4} - 8.7 \times 10^{-4}$ mol/L. Caffeine concentration of energy drinking water is in agreement with the declared content (i.e., 200 mg/L).

Sample	DPV value	UV–vis spectroscopic value
Cola beverage1	$6.2 \pm 0.53 \times 10^{-4}$ mol/L	$6.1 \pm 0.29 \times 10^{-4}$ mol/L
Cola beverage 2	$5.3 \pm 0.16 \times 10^{-4}$ mol/L	$5.2 \pm 0.53 \times 10^{-4}$ mol/L
Energy drinking water	200 ± 10 mg/L	198 ± 14 mg/L
Green tea	28.9 ± 0.42 mg/g	29.6 ± 0.25 mg/g

Table 1. Results obtained in determination of caffeine in beverage samples and tea using the DPV (proposed) and UV–vis spectroscopic methods (n = 5) .

The content of TP in theophylline sustained-release tablet was calculated to be 0.0921g per tablet (the declared content was 0.1 g per tablet); the content of TP in aminophylline injection was calculated to be 0.1976 g per ampoule (the declared content was 0.2 g per ampoule). The determined contents of TP were in agreement with the declared contents of TP in real samples. The results demonstrated that the proposed methods could be efficiently used for the determination of caffeine and TP.

3. CNTs modified electrode used in analysis of weak acidic pharmaceuticals

Ascorbic acid (AA) is widely present in many biological liquids, medicines, fruits and beverages. It is one of the most important soluble vitamins and plays a significant role in the biological functioning, such as the supplement of inadequate dietary intake，wound healing [15, 16], prevention as well as treatment of common cold, mental illness and infertility [17]. Uric acid (UA) is one of the principal end products of purine metabolism in human body. Abnormal levels of UA are symptoms of several diseases, like gout, hyperuricaemia and Lesch–Nyhan syndrome [18]. Hence, monitoring the concentration of UA in biological fluids has their clinical significance. Generally, AA and UA always coexist in biological fluids such as blood and urine, and AA has a close oxidation peak potential of UA, which results in poor selectivity determination of AA or UA in real samples on conventional electrodes. Therefore, it is essential to exploit more sensitive, selective and simple methods for the simultaneous determination of AA and UA. Recently, our group

has realized the simultaneous determination of AA and UA using Nafion/CNTs composite film-modified electrode [19].

Figure 3A demonstrated the cyclic voltammetry (CV) curves of a mixture of UA and AA (containing 8.0×10^{-5} mol/L UA and 1.0×10^{-3} mol/L AA) (a), 1.0×10^{-3} mol/L AA (b) and without AA and UA (c) in 0.1 mol/L NaCl (pH 6.5) at Nafion/CNTs/GCE, respectively.

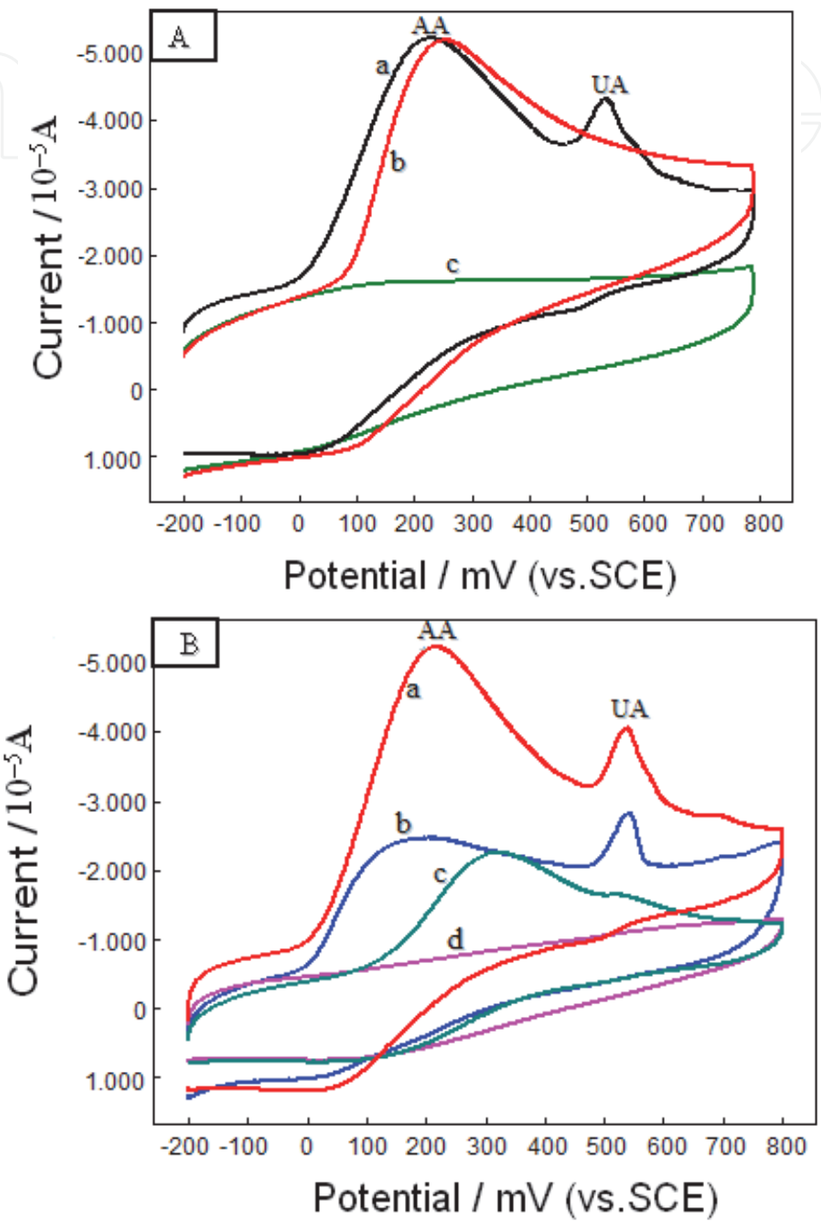

Fig. 3. (A) CV curves of the mixture containing 1.0×10^{-3} mol/L AA and 8.0×10^{-5} mol/L UA (a), 1.0×10^{-3} mol/L AA (b) and without AA and UA (c) in 0.1 mol/L NaCl solution (pH 6.5) at the Nafion/CNTs/GCE; (B) CV curves of the mixture containing 1.0×10^{-3} mol/L AA and 8.0×10^{-5} mol/L UA in 0.1 mol/L NaCl solution (pH 6.5) at the Nafion/CNTs/GCE (a), CNTs/GCE (b), bare GCE (c) and Nafion/GCE (d); scan rate: 100 mV/s, rest time: 3 s

Figure 3A-a showed two anodic peaks at around the potential of 534 and 214 mV, which attributed to the oxidation of UA and AA with a 320 mV separation of both peaks. Figure 3B revealed CV response of a mixture of UA and AA (containing 8.0×10^{-5} mol/L UA and 1.0×10^{-3} mol/L AA) in 0.1 mol/L NaCl (pH 6.5) at Nafion/CNTs/GCE (a), CNTs/GCE (b), bare GCE (c) and Nafion/GCE (d). Under the same conditions, no anodic peak of AA or UA was observed at the Nafion/GCE. At the bare GCE, UA and AA exhibited an overlapped and broad anodic peak extended over a potential region of 98–580 mV with the mixed potential at 310 mV. However, CV for the Nafion/CNTs/GCE and CNTs/GCE showed two anodic peaks with a separation of about 320 mV towards UA and AA, which was broad enough for their simultaneous electrochemical determination. Nevertheless，at the Nafion/CNTs nanocomposite-modified electrode, the peak currents were significantly higher than those at the CNTs/GCE or the bare GCE.

Under the optimized conditions, the peak currents of AA and UA were proportional to their concentration at the ranges of 8.0×10^{-5} to 6.0×10^{-3} mol/L and 6.0×10^{-7} to 8.0×10^{-5} mol/L, respectively. The proposed method was used for the detection of AA and UA in real samples, such as Vitamin C Injection and urine sample.

The total value of AA in Vitamin C Injection was 242 g/L. The total value of AA was in agreement with the declared content (i.e., 250 g/L). The total UA concentrations detected in urine sample was 4.37×10^{-3} mol/L, which was consistent with the containing level of a healthy human. The results demonstrated that the proposed methods could be efficiently used for the determination of AA and UA.

Paeonol (2-hydroxyl-4-methoxyacetophone, PN) is a major phenolic component of Cortex Moutan. It is known to have anti-aggregatory, anti-oxidant and anti-inflammatory activities [20]. Paeonol has been used in the treatment of arthritis and suppress ADP- or collagen-induced human blood platelet aggregation in a dose-dependent manner due to its analgesic, anti-pyretic, and anti-bacterial properties [21]. Many researchers have given increasing attention to the pharmacokinetic activities of paeonol. Therefore, the technique of quantitative determination of paeonol is crucial to the evaluation and popularization of traditional Chinese medicines as well as drug products containing paeonol [22, 23]. We have carried out the determination of paeonol in pharmaceutical and biological samples using Nafion/CNTs-modified electrode as a sensitive voltammetric sensor [24].

As shown in figure 4, paeonol exhibited an anodic peak on the Nafion/CNTs/GCE (Figure 4-a), Nafion/GCE (Figure 4c) and a bare GCE (Figure 4-b) in 0.1 mol/L phosphate buffer solution (pH 7.0). According to Wang's report [25], paeonol was easy to yield compact insulated polymer arylether on the bare electrode surface, which could prevent the progression of the electrode reaction on the electrode surface. Nafion, a perfluorinated sulfonate polymer is a good cation-exchanger provided with adsorption ability and high surface area. It maybe effectively prevents the macro-polymer arylether adsorbing on the modified electrode surface and avoid anode fouling by forming a dense film with a low permeability. Thus, when Nafion was present, the anodic peak current (i_{pa}) was effectively separated from the background current (curve c). When Nafion and CNTs were combined together, the peak potential moved in the negative direction slightly at about 836 mV (vs. SCE) with the obvious enhancement of the peak current (curve a). This phenomenon maybe related to the influence of CNTs on the electron transfer rate, the effective electrode area, as well as the accumulation amount of paeonol. The resulting composite materials coated electrode exhibited more sensitive response to paeonol, meaning that composite materials

could cooperate with each other to enhance the voltammetric response of paeonol. In addition, it was observed that paeonol also produced a slight cathodic peak at about 440 mV (vs. SCE) on the Nafion/CNTs/GCE, which indicated that Nafion/CNTs/GCE was much more sensitive than Nafion/GCE in improving paeonol response under the same conditions.

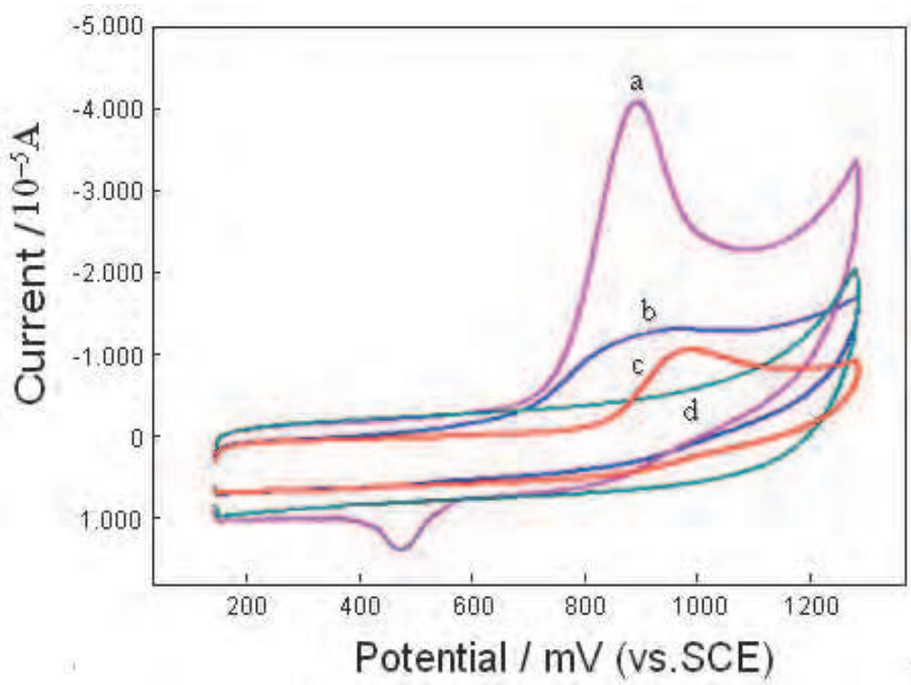

Fig. 4. Cyclic voltammograms on the Nafion/CNTs-modified GCE (a), the bare GCE (b), Nafion-modified GCE (c) containing 8.0×10^{-5} mol/L paeonol and Nafion/CNTs-modified GCE (d) without paeonol in 0.1 mol/L NaH_2PO_4– Na_2HPO_4 (pH 7.0) medium; scan rate 100 mV/s.

The relationship between the anodic peak current and the concentration of paeonol was studied using differential pulse anodic stripping voltammetry. Under the optimum instrumental conditions, the anodic peak current was proportional to paeonol concentration in the range of 6.0×10^{-7}– 6.0×10^{-5} mol/L with a detection limit of 4.0×10^{-7} mol/L. The Nafion/CNTs/GCE was applied to the determination of paeonol in Liuweidihuang Wan and Cortex Moutan and the results were listed in Table 2. Total value of paeonol in Liuweidihuang was 3.20 ± 0.75 mg/g, which was close to the revealed value of 3.22 mg/g [26]. Total value of paeonol in cortex moutan was 20.05 ± 0.50 mg/g, which was consistent with the reported value of 20.61 ± 0.986 mg/g [27]. The accuracy of the method was evaluated by its recovery during spiked experiments. Confirming those quantitative and reproducible results of this method, the direct determination of paeonol in spiked Liuweidihuang Wan, Cortex Moutan, urine and plasma samples were carried out, and the results were also displayed in Table 2. The recoveries of paeonol from the drug matrices and biological samples, such as urine and plasma demonstrated that this proposed method could be applied to the detection of paeonol in pharmaceutical and biological samples with excellent sensitivity and selectivity.

Sample	Original (μmol/L)	Spike (μmol/L)	Found (μmol/L)	Average recovery (%)	RSD of recovery (%)
LiuweidihuangWan[a]	7.71 ± 0.19	40	47.52 ± 0.52	98.7	2.3
		8	15.83 ± 0.24	101.5	2.0
		2	9.63 ± 0.17	96.0	1.5
Cortex Moutan[b]	48.26 ± 0.24	40	88.10 ± 0.21	99.6	2.0
		8	57.92 ± 0.23	108.2	3.2
		2	50.30 ± 0.14	102.0	2.3
Urine[c]	—	80	79.80 ± 0.31	99.8	2.6
		20	20.25 ± 0.10	101.3	1.7
		2	1.99 ± 0.22	99.5	1.9
Plasma[c]	—	80	81.20 ± 0.42	101.5	3.0
		20	21.00 ± 0.19	105.0	3.7
		2	1.96 ± 0.20	98.0	2.2

Table 2. Determination of the content of paeonol in pharmaceutical and biological samples∗ on the Nafion/CNTs/GCE.
a Dilution factor: 1/100.
b Dilution factor: 1/10.
* Number of samples assayed: 5.

4. CNTs with methylene blue composite film-modified electrode for the simultaneous voltammetric detection of dopamine and uric acid in the presence of high concentration of ascorbic acid

Dopamine (DA) as one of the most important catecholamines, is an significant neurotransmitter and plays a vital role in the central nervous, renal, hormonal and cardiovascular systems [28, 29]. Inadequate DA-containing neurons may cause neurological disorders such as schizophrenia and Parkinson's disease [30]. Therefore, determining the concentration of this neurochemical is of great clinical importance. Uric acid (UA) is one of the principal end products of purine metabolism in the human body. Hence, monitoring the concentration of UA in biological fluids has their clinical significance. Electrochemical methods can be used to determine DA and UA due to their electrochemical active. But the significant problem encountered with the detection of DA or UA using electrochemical methods arising from the primary interference of ascorbic acid (AA). Generally, AA, DA and UA always coexist in biological fluids, and AA has an overlapping oxidation peak of DA and UA at bare electrodes, which results in poor selectivity determination of DA or UA in real samples. Therefore, it is essential to eliminate the interference of AA by using suitable film-modified electrode for the selective determination of DA and UA.
Through the adsorption of methylene blue (MB) onto the CNTs, our group has successfully prepared a sensitive voltammetric sensor CNTs/MB for the selective determination of DA and UA [31]. In order to ascertain the formation of MB-CNTs nanostructure, UV-vis spectral measurements, atomic force microscope (AFM), scanning electron microscopy (SEM) and electrochemical impedance spectra (EIS) were carried out.

As shown in figure 5, the absorption spectra of water-dispersed solutions of free MB (curve a), CNTs (curve b) and the MB-CNTs adduct (curve c) were displayed. The UV-vis spectrum of the CNTs dispersed in aqueous solution exhibited a strong absorbance at 263 nm. The spectrum of free MB in aqueous solution displayed two strong absorption peaks at 294 and 665 nm (curve a), characteristic of the MB monomer in solution. The chemisorption of MB onto the CNTs was evident from the spectrum of the MB-CNTs composite (curve c), which was similar to that of CNTs. However, a close inspection of the spectrum of CNTs and the MB-CNTs adsorptive nanostructure revealed that there was a change in the spectrum of CNTs after its adsorption of MB. A new peak appeared at 690 nm was observed, which was due to the absorbance of the aggregation of MB molecules onto the CNTs [32].

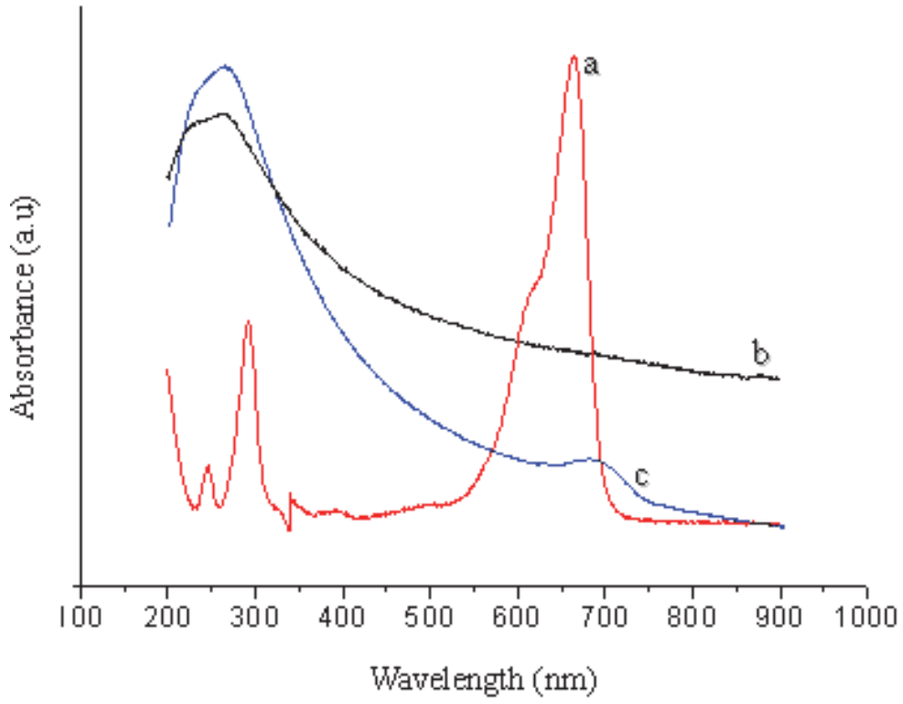

Fig. 5. Absorption spectrum of aqueous dispersion of MB (a), aqueous dispersion of CNTs (b), and aqueous dispersion of MB-CNTs (c).

Figure 6 presented the morphology of CNTs (Figure 6 A, B) and MB-CNTs (Figure 6 C, D) powder samples on a mica sheet, obtained by an atomic force microscope (AFM). The powder samples showed the existence of CNTs in a network-like structure with an unorderly arrangement. The adsorption of MB on CNTs seemed to break the intertwined network of CNTs into individual carbon nanotubes. In addition, some breaking and shortening of CNTs into smaller ones were obvious. The average diameter of individual strand of CNTs was about 38.05 nm. The average diameter of individual strand of MB-CNTs was about 62.03 nm, which was nearly twice that of CNTs indicating clearly that the individual strand of CNTs was entirely encapsulated or wrapped by the MB to form a tubular composite. Moreover, the MB-CNTs sample could be readily dispersed in water to give a black-colored solution, but the CNTs couldn't be easily dissolved or dispersed in aqueous solution. This observation again indicated an adsorption of MB on CNTs.

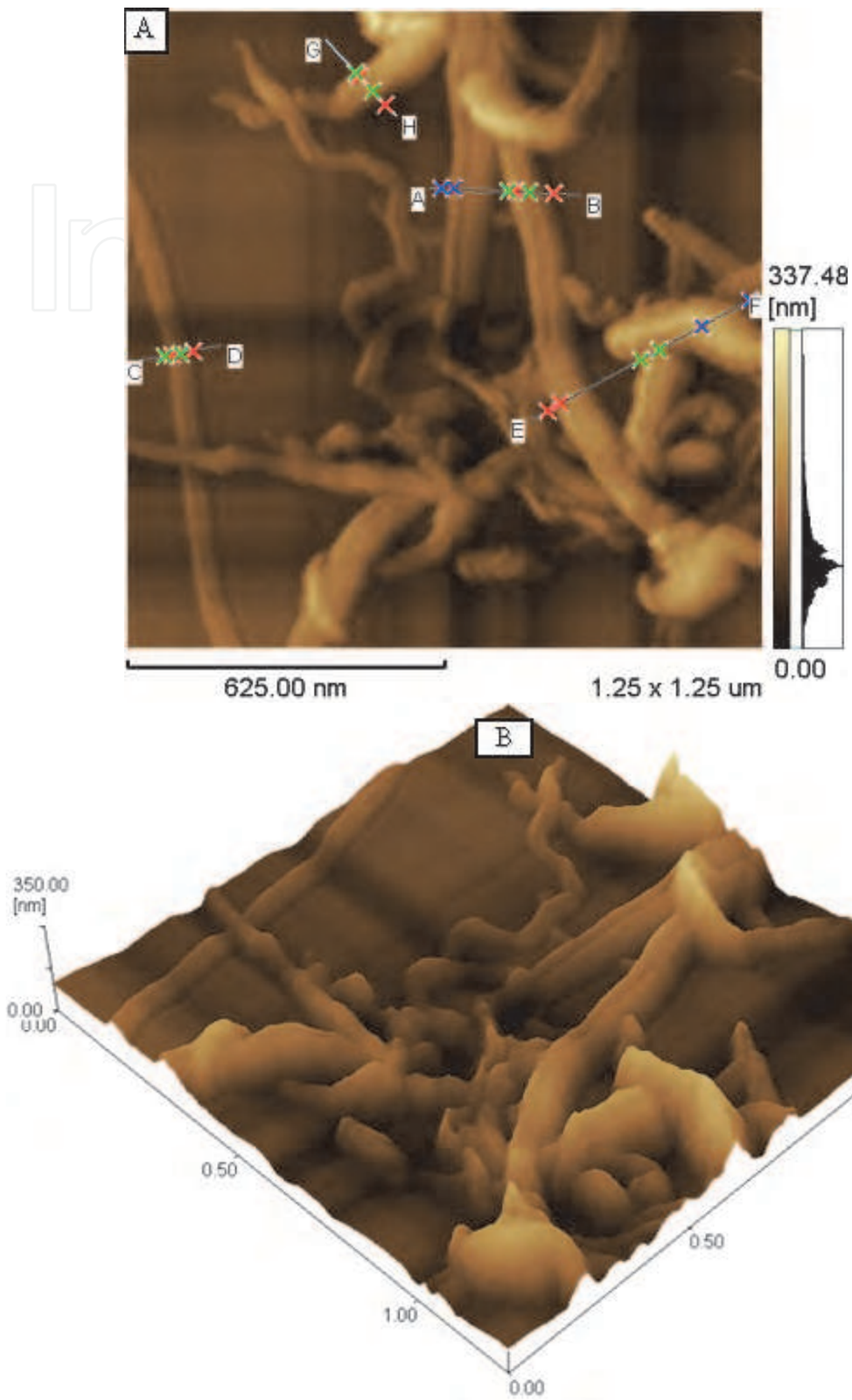
A
G
H
A
B
337.48
[nm]
F
C
D
E
0.00
625.00 nm
1.25 x 1.25 um
B
350.00
[nm]
0.00
0.00
0.50
1.00
0.50
1.00
0.00

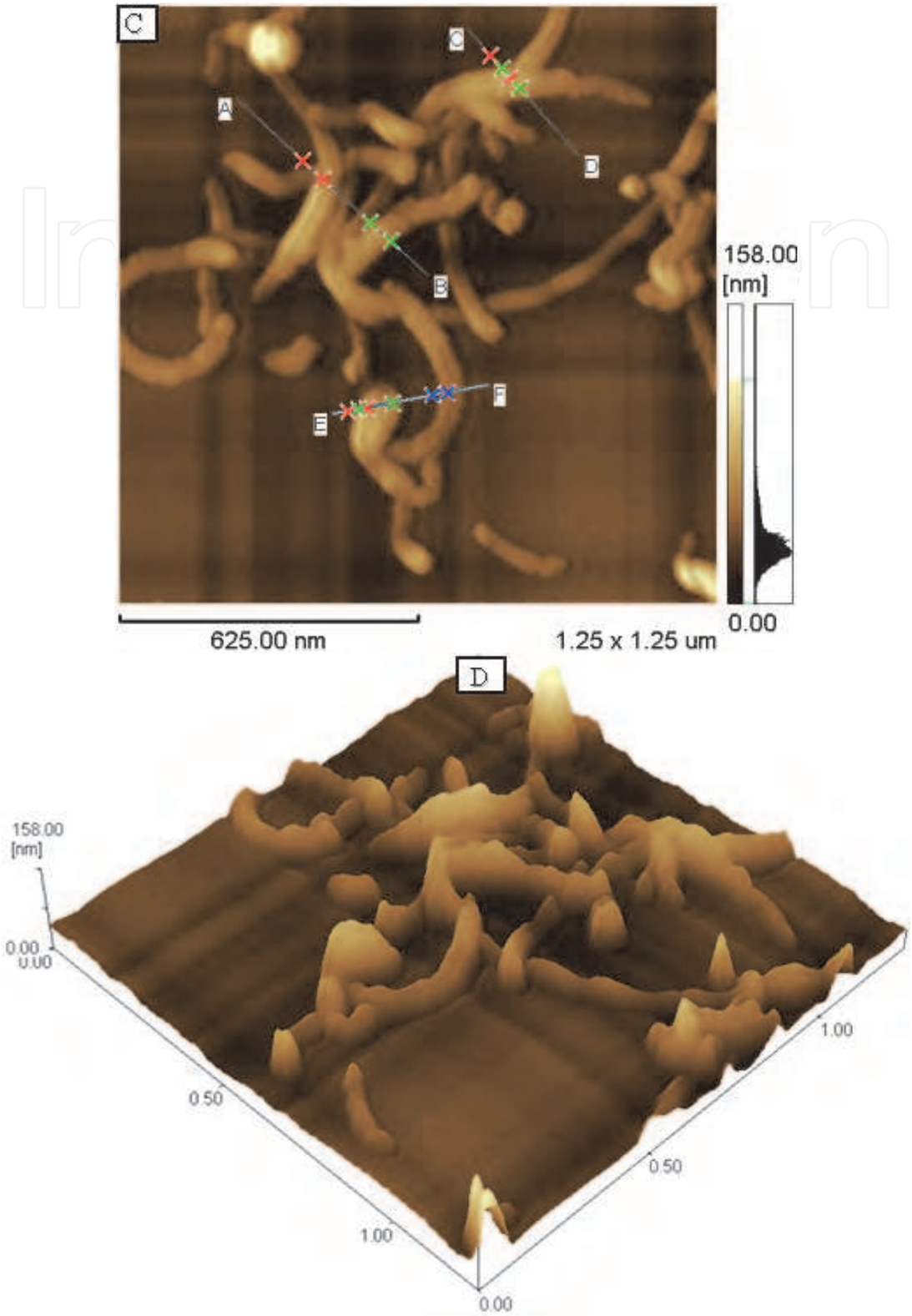

Fig. 6. AFM image of CNT (A, B) and MB-CNTs (C, D) power samples on a mica sheet.

Figure 7 demonstrated cyclic voltammograms of the CNTs/GCE (curve a) and MB-CNTs/GCE (curve b) immersed into 0.1 mol/L pure phosphate buffer (pH 3.0) containing no MB. There was no any redox wave of CNTs/GCE in the potential range of -400–600 mV. In contrast to CNTs/GCE, a pair of redox waves of the MB-CNTs/GCE was observed at 95 and 27 mV, suggesting that electroactive MB can adsorb onto the CNTs and form an electrochemically functional nanostructure.

Figure 8 showed the results of the electrochemical impedance spectra (EIS) of a bare GCE, CNTs/GCE and MB-CNTs/GC electrode in a solution containing 0.1 mol/L KCl and 1.0 mmol/L $Fe(CN)_6^{3-/4-}$. The Nyquist plot exhibited a poor small semicircle portion at higher frequencies, and a line at lower frequencies for the bare GCE (Figure 8A), which was similar to the characteristic of a diffusion limiting step of the electrochemical process. However, at CNTs/GCE, the Nyquist plots displayed a clear bigger semicircular feature in addition to the linear feature (Figure 8B-a). The semicircle portion, as observed at higher frequencies, was associated with a process that was limited by electron transfer. The linear features observed at lower frequencies were attributed to diffusion-limited electron transfer. Adsorption of MB on the CNTs to fabricate MB-CNTs/GCE caused a remarkably decrease of the semicircle portion at higher frequencies to form a nearly-straight line (Figure 8B-b). This may be demonstrated that MB-CNTs film introduced an advantage to the interfacial electron transfer. Because of the positive charge of MB in the film, the $[Fe(CN)_6]^{4-/3-}$ probe could arrive to the surface of the electrode promptly. The impedance changes of the different modified electrodes revealed that MB had adsorbed on the CNTs.

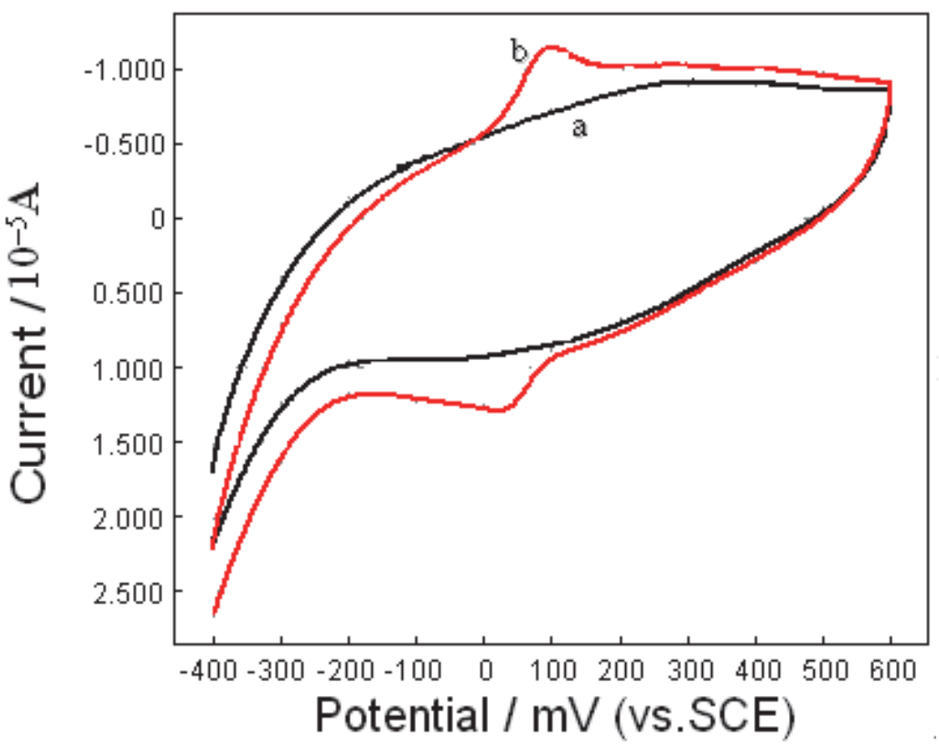

Fig. 7. Cyclic voltammograms of the CNTs/GCE (a) and MB-CNTs/GCE (b) in 0.1 mol/L phosphate buffer (pH 3.0); scan rate 80 mV/s

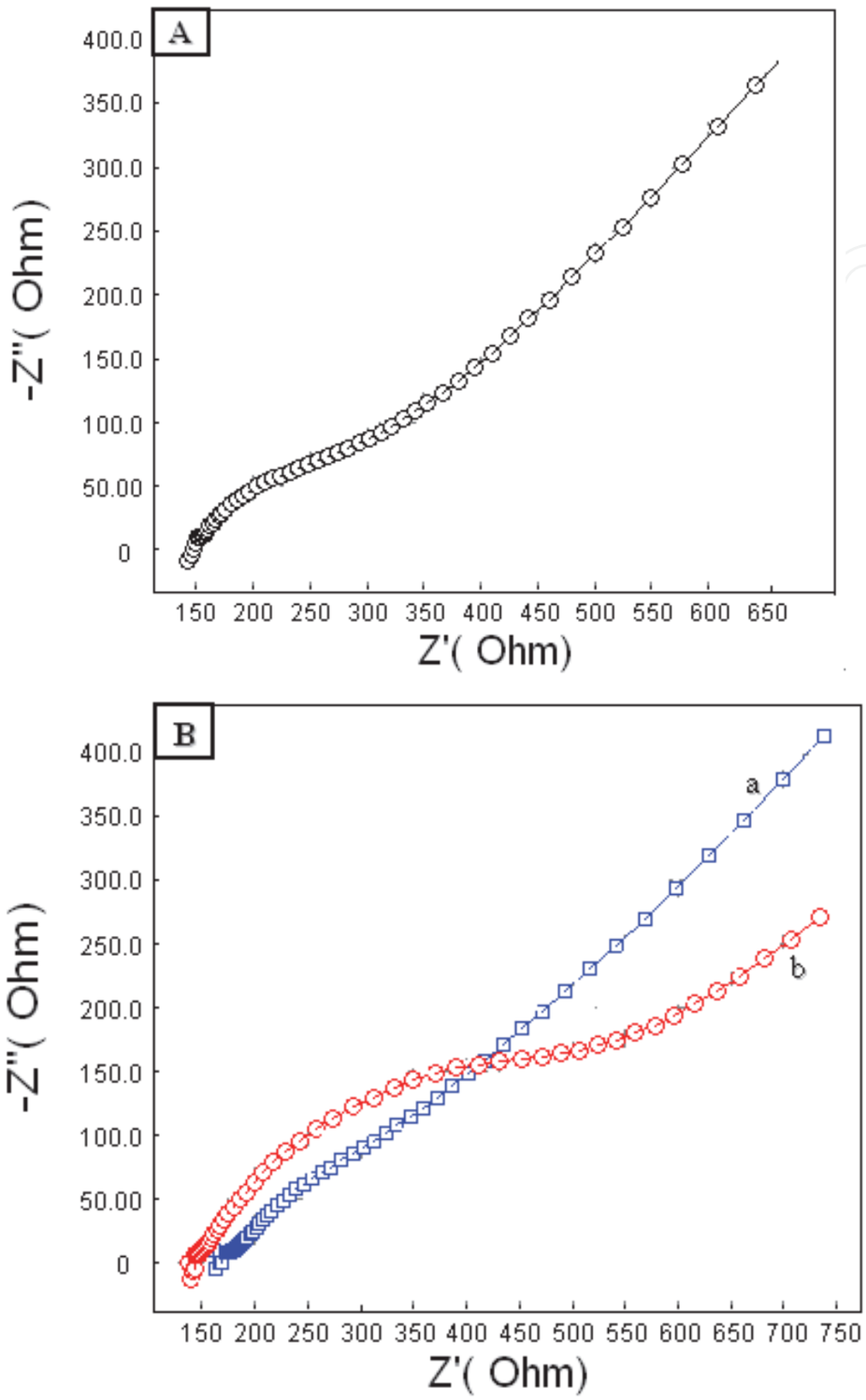

Fig. 8. (A) Nyquist diagram of EIS at bare GCE; (B) Nyquist diagrams of EIS at MB-CNTs/GCE (a) and CNTs/GCE (b). EIS condition: frequency range: 100 kHz–1 Hz; signal amplitude: 5 mV; solution: 1.0 mmol/L $Fe(CN)_6^{3-/4-}$ in 0.1 mol/L KCl.

The modified electrode showed excellent electrocatalytic activity toward dopamine (DA) and uric acid (UA) in 0.1 mol/L phosphate solution medium (pH 3.0). Figure. 9A demonstrated the cyclic voltammetry (CV) curves of a mixture of 3.0×10^{-4} mol/L DA and 6.0×10^{-4} mol/L UA (a), 3.0×10^{-4} mol/L DA (b), 6.0×10^{-4} mol/L UA (c), and buffer solution without DA and UA (d) in 0.1 mol/L phosphate solution (pH 3.0) at MB-CNTs/GCE, respectively. Figure. 9A-a showed two anodic peaks at around the potential of 429 and 603 mV, which attributed to the oxidation of DA and UA with a 174 mV separation of both peaks, which was broad enough for their simultaneous electrochemical determination of DA and UA. Figure 9B revealed CV responses of a mixture of 3.0×10^{-4} mol/L DA and 6.0×10^{-4} mol/L UA in 0.1 mol/L phosphate solution (pH 3.0) at MB-CNTs/GCE (a), CNTs/GCE (b), bare GCE (c) and MB/GCE (d). Under the same conditions, poor anodic peaks of DA and UA were observed at the bare GCE. At the MB/GCE, DA and UA exhibited an overlapped and broad anodic peak extended over a potential region of 450–630 mV with the mixed potential at 530 mV. CV for CNTs/GCE showed two anodic peaks with a separation of about 144 mV towards DA and UA. Comparing MB-CNTs/GCE with CNTs/GCE, a remarkable increase in redox peak currents of DA was observed with the anodic potential shift negatively (more than 30 mV), which revealed that MB in the matrix of CNTs/GCE can act as an efficient electron mediator for the electrocatalytic oxidation of DA，besides CNTs can enhance the electron-transfer rate and make more DA participate in the electrochemical reaction due to their accumulation and catalytic ability. The anodic (E_{pa}) and cathodic peak potentials (E_{pc}) of DA were at about 429 mV and 336 mV (vs. SCE), respectively, and the peak currents ratio of i_{pa}/i_{pc} was about 1.0, which showed that the electrode reaction of DA was almost reversible.

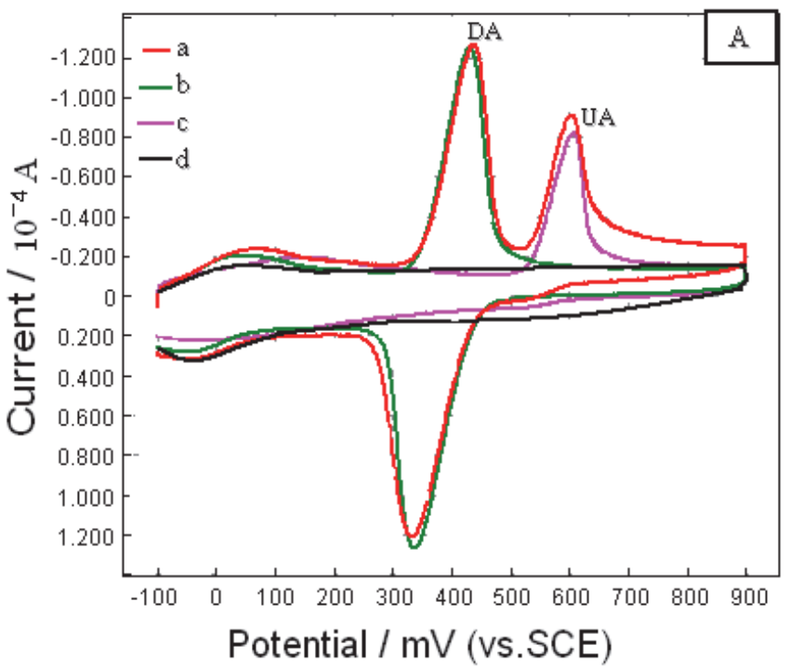

Fig. 9. (A) CV curves of the mixture containing 3.0×10^{-4} mol/L DA and 6.0×10^{-4} mol/L UA (a), 3×10^{-4} mol/L DA (b), 6×10^{-4} mol/L UA (c), and buffer solution without DA and UA (d) in 0.1 mol/L phosphate solution (pH 3.0) at the MB-CNTs/GCE.

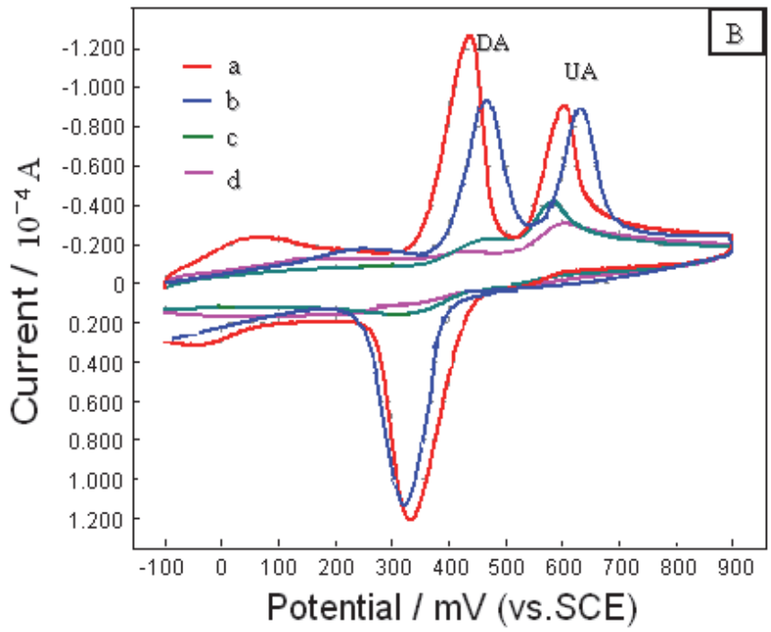

Fig. 9. (B) CV curves of the mixture containing 3.0 × 10^{-4} mol/L DA and 6.0 × 10^{-4} mol/L UA in 0.1 mol/L phosphate solution (pH 3.0) at different modified electrodes: MB-CNTs/GCE (a), CNTs/GCE (b), bare GCE (c), and MB/GCE (d); scan rate 80 mV/s.

Generally, as the electroactive substance, ascorbic acid (AA) always coexists with DA and UA. The oxidation peak potential of AA is very close to that of DA and UA, which results in poor selectivity determination of DA or UA in real samples on conventional electrodes. Therefore, it is essential to exploit more sensitive, selective and simple methods for the segregative determination of AA, DA and UA. Figure 10 demonstrated the differential pulse anodic stripping voltammetry (DPASV) curves of the mixture of 3.0 × 10^{-4} mol/L DA and 6.0 × 10^{-4} mol/L UA (a), 3.0 × 10^{-3} mol/L AA, 3.0 × 10^{-4} mol/L DA and 6.0 × 10^{-4} mol/L UA (b), 1.0 × 10^{-3} mol/L AA, 3.0 × 10^{-4} mol/L DA and 6.0 × 10^{-4} mol/L UA (c), 1.0 × 10^{-3} mol/L AA (d) and 0.1 mol/L phosphate buffer solution (pH 3.0) (e) in 0.1 mol/L phosphate buffer solution (pH 3.0) on MB-CNTs/GCE. Figure 10-d showed an anodic peak at around 200 mV, which was attributed to the oxidation of AA, the separation potential of AA and DA was about 219 mV, indicating broad enough separation to eliminate the interference of AA and realize the simultaneous electrochemical determinations of DA and UA in the mixed solution.

Under the optimized conditions, In the presence of 1.0 mmol/L AA and 10.0 μmol/L UA, the anodic peak current was linear to the concentration of DA in the range of 0.4−10.0 μmol/L with a detection limit of 0.2 μmol/L DA. The anodic peak current of UA was linear to the concentration in the range of 2.0−20.0 μmol/L and 20.0−200.0 μmol/L with a lowest detection limit of 1.0 μmol/L in the presence of 1.0 mmol/L AA and 1.0 μmol/L DA.

The repeatability and stability are the vital characteristics for the modified electrode, which should be investigated for analytical determination. The same MB-CNTs/GCE was used for five times successive measurement, and the relative standard deviation (RSD) of the peak current was 3.5 % for 3.0 × 10^{-4} mol/L DA and 4.0 % for 6.0 × 10^{-4} mol/L UA. In addition, five freshly prepared MB-CNTs/GCE were used to measure 3.0 × 10^{-4} mol/L DA in the same condition. All five electrodes exhibited similar current responses and a relative

standard deviation of 5.6% was obtained. These findings revealed that the electrochemical behavior of the MB-CNTs/GCE was highly repeatable. The stability of the MB-CNTs/GCE was studied by determining the steady-state response current of 3.0 × 10^{-4} mol/L DA every day after preparation, the RSD of steady-state response current was 6.5%. When not in use, the sensor was stored in 0.1 mol/L PBS buffer (pH 7.0) at 4 °C. The results showed that the steady-state response current only decreased by 12% after 7 days, indicating that the MB-CNTs/GCE electrode was considerably stable.

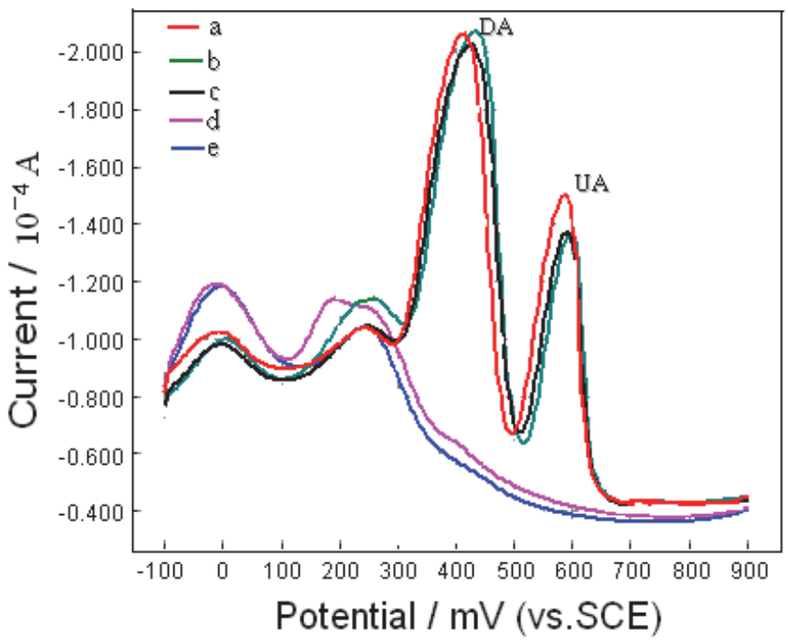

Fig. 10. Differential pulse anodic stripping voltammograms of the mixed solution of 3.0 × 10^{-4} mol/L DA and 6.0 × 10^{-4} mol/L UA (a), 3.0 × 10^{-3} mol/L AA, 3.0 × 10^{-4} mol/L DA and 6.0 × 10^{-4} mol/L UA (b), 1.0 × 10^{-3} mol/L AA, 3.0 × 10^{-4} mol/L DA and 6.0 × 10^{-4} mol/L UA (c), 1.0 × 10^{-3} mol/L AA (d) and 0.1 mol/L phosphate buffer solution (pH 3.0) (e) on the MB-CNTs/GCE; instrument parameters: accumulation time: 40 s, accumulation potential: 100 mV, pulse amplitude: 50 mV, pulse increment: 4 mV, pulse width: 40 ms and pulse period: 120 ms.

The MB-CNTs/GCE electrode was used in real samples analysis, such as Dopamine Hydrochloride Injection and urine. The detected results were shown that the total value of DA in Dopamine Hydrochloride Injection was 10.48 mg/mL, which was in agreement with the declared content (i.e., 10.0 mg/mL). The total UA concentrations detected in urine sample was 4.54 × 10^{-3} mol/L, consistent with the containing level of a healthy human.

5. Gold nanoparticles/ethylenediamine/carbon nanotubes-modified glassy carbon electrode as the voltammetric sensor for selective determination of rutin in the presence of ascorbic acid

Rutin (3′, 4′, 5, 7-tetrahydroxyflarone-3β-d-rutinoside), as a kind of the most abundant bioactive flavonoid called as vitamin p, is widely present in multivitamin preparations and more than 70 herbal remedies. As a natural flavone derivative, rutin has a wide range of

physiological activities including anti-inflammatory, hemostat, antibacterial anti-tumor and anti-oxidant [33–35]. It is always used clinically as the therapeutical medicine [36, 37]. For example, It can be applied to the treatment of diseases, such as capillary bleeding by diluting the blood, reducing capillary permeability and lower blood pressure [38]. Hence, it is necessary to develop simple, sensitive, economical and efficient techniques for the determination of rutin. Recently, we reported a preparation and application of AuNPs/en/CNTs composite film-modified glassy carbon electrode (AuNPs/en/CNTs/GCE) [39].

SEM can effectively prove the surface morphologies of the modified electrode. The morphology of the CNTs film (Figure 11-a) showed a network-like structure. Compared with the CNTs film, the SEM image of AuNPs/en/CNTs films (Figure 11-b) displayed many observable light dots which were due to the assembly of AuNPs. SEM image (Figure 11-b) confirmed that gold nanoparticles were typically bound on CNTs with fairly even distribution, although a few aggregates were observed.

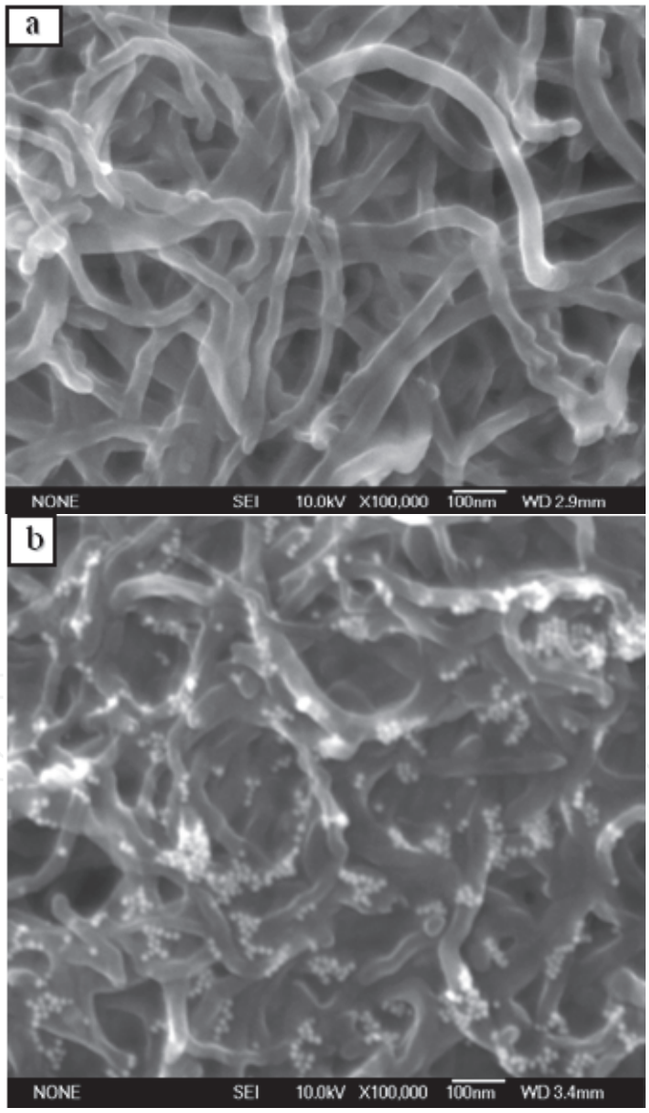

Fig. 11. SEM images of CNTs film (a), and AuNPs/en/CNTs films (b)

Experiments revealed that the redox peak currents of rutin could be remarkably enhanced on AuNPs/en/CNTs/GCE, meaning good electrocatalytic activity for the oxidation of rutin. Figure 12 showed the cyclic voltammograms of rutin on different modified electrodes. Rutin didn't display any redox peaks at the bare GCE (a), which demonstrated the weaker adsorption and slower electrochemical reaction of rutin on the GCE surface. However, there were well-defined redox peaks on the en/CNTs/GCE (b), CNTs/GCE (c) and AuNPs/en/CNTs/GCE (d) in 0.1 mol/L phosphate buffer solution (pH 3.5). But the heights of the redox peaks were clearly higher in the case of AuNPs/en/CNTs/GCE than that of the redox peaks on the en/CNTs/GC or CNTs/GCE. The anodic (E_{pa}) and cathodic peak potentials (E_{pc}) were at about 487 mV and 432 mV (vs. SCE), respectively, and the ratio of i_{pa}/i_{pc} was about 1.2, which showed that the electrode reaction was almost reversible. Nano-gold and CNTs can enhance the electron-transfer rate and make more rutin participate in the electrochemical reaction due to their accumulation and catalytic ability.

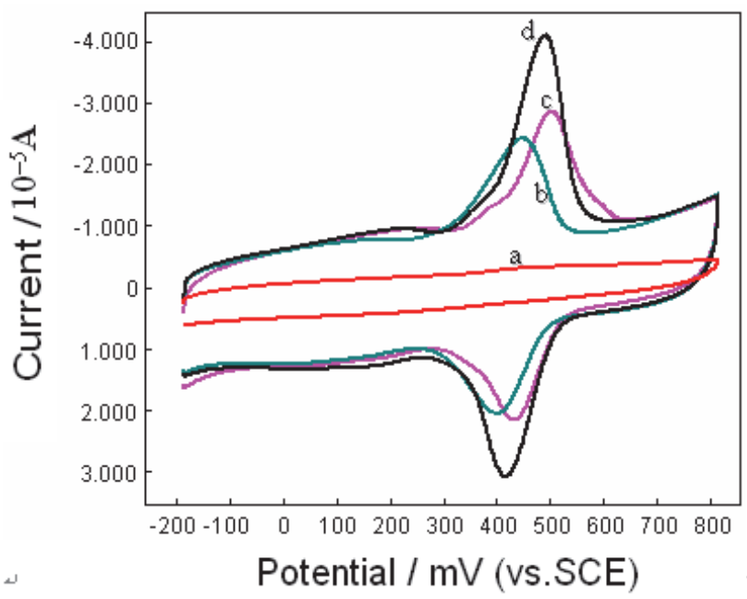

Fig. 12. Cyclic voltammograms of 8.0×10^{-5} mol/L rutin in 0.1 mol/L phosphate buffer (pH 3.5) on the different electrodes: the bare GCE (a), en/CNTs /GCE (b), CNTs/GCE (c) and AuNPs/en/CNTs/GCE (d); scan rate 100 mV/s.

Generally, as the electroactive substance, ascorbic acid (AA) always coexists in the Compound Rutin Tablets. The oxidation peak potential of AA is very close to that of rutin, which results in poor selectivity determination of AA or rutin in real samples on conventional electrodes. Therefore, it is essential to exploit more sensitive, selective and simple methods for the segregative determination of AA and rutin. Figure 13 demonstrated the cyclic voltammetry (CV) curves of 1.0×10^{-4} mol/L AA (a), the mixture of 2.0×10^{-5} mol/L rutin and 1.0×10^{-4} mol/L AA (b), 2.0×10^{-5} mol/L rutin (c) and without AA and rutin (d) in 0.1 mol/L phosphate buffer solution (pH 3.5) on AuNPs/en/CNTs/GCE. Figure 13 b showed two anodic peaks at around 186 mV and 487 mV, which were attributed to the oxidation of AA and rutin with a 301 mV separation of both peaks, indicating broad enough separation for the simultaneous electrochemical determinations of rutin and AA in the mixed solution.

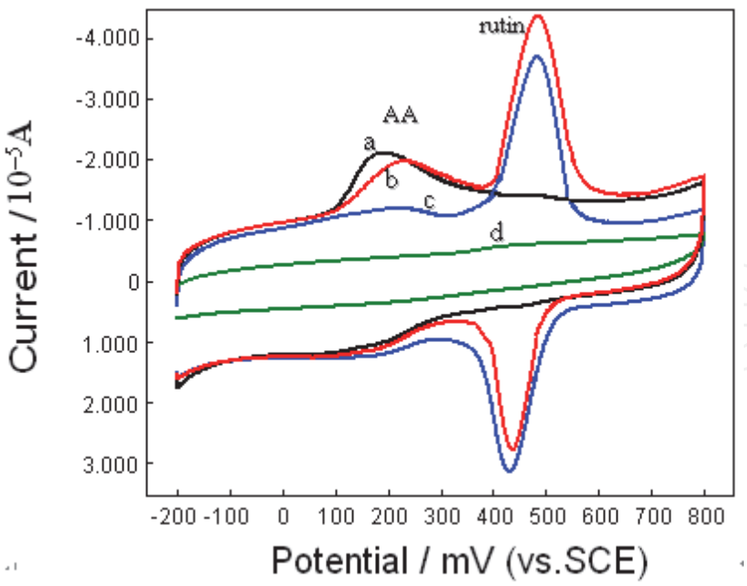

Fig. 13. Cyclic voltammograms of 1.0×10^{-4} mol/L AA (a), the mixed solution of 1.0×10^{-4} mol/L AA and 2.0×10^{-5} mol/L rutin (b), 2.0×10^{-5} mol/L rutin (c) and 0.1 mol/L phosphate buffer solution (pH 3.5) (d) on the AuNPs/en/CNTs/GCE; scan rate 100 mV/s.

Under optimized conditions, the anodic peak current was linear to the rutin concentration in the range of 4.8×10^{-8} mol/L − 9.6×10^{-7} mol/L. The regression equation was: $i_{pa} = 2.3728 C_{rutin} - 0.1782$ (i_{pa}: 10^{-5}A, C_{rutin}: μmol/L, $r = 0.9973$). The detection limit of 3.2×10^{-8} mol/L was obtained. Regeneration and reproducibility are two important characteristics for the modified electrode, which should be investigated. The same modified GCE was used for six times successive measurements of 2.0×10^{-5} mol/L rutin. After each measurement, the surface of the AuNPs/en/CNTs/GCE was regenerated by successively cycling between -200 mV and 800 mV (vs. SCE) in 0.1 mol/L phosphate buffer solution (pH3.5) for six cycles. The relative standard deviation (RSD) of the anodic peak current was 4.3%, which suggested good regeneration and reproducibility of the modified electrode.

This method was used for the determination of rutin in the Compound Rutin Tablets and Rutin Tablets. The contents of rutin in the Compound Rutin Tablets and Rutin Tablets were calculated to be 20.0 ± 0.87 mg and 19.4 ± 0.54 mg per tablet, respectively (the declared content of rutin was 20 mg per tablet). In order to test the accuracy of the proposed method, the conventional method of HPLC was employed to determine the contents of rutin in the Compound Rutin Tablets and Rutin Tablets (the contents of rutin in the Compound Rutin Tablets and Rutin Tablets were 18.9 ± 0.47 mg and 18.1 ± 0.57 mg per tablet, respectively). The quantitative results obtained by HPLC were in agreement with the data determined by the proposed electrochemical method, indicating that the method was selective and suitable for rutin determination in real samples.

6. Preparation of yttrium hexacyanoferrate/carbon nanotube/Nafion nanocomposite film-modified electrode: Application to the electrocatalytic oxidation of L-cysteine

L-cysteine (L-CySH), a sulfur-containing molecule, is one of the most important amino acids. It is widely present in many medicines, food and biological tissues, such as cysteine

protease, vasopressin and anti-diuretic hormone [40]. It plays a significant role in biological systems, playing a role in folding and defolding mechanisms [41]. An inadequate dietary intake of L-CySH may cause number of clinical problems, for instance, liver damage, skin lesions, and slowed growth [42]**.** Therefore, the sensitive detection of L-CySH is clinically significant. Nevertheless, some traditional methods, such as the chromatographic methods, are time-consuming, expensive, and require complicated preconcentration, multisolvent extraction and trained technicians. In contrast, electrochemical methods are characterized by their simplicity, high sensitivity, good stability, low-cost instrumentation, small scale and on-site monitoring [43]. However, although L-CySH is an electroactive compound, there are some drawbacks in electroanalysis, for example, large overpotential, low sensitivity and sluggish electron-transfer kinetics at conventional electrodes. These obstacles can result in oxide formation and fouling of the electrode surface [44]. To overcome these obstacles, we have successfully prepared YHCFNP, and the electrocatalytic oxidation and amperometric determination of L-CySH were accomplished at a modified electrode compose of a mixture of YHCFNP and CNTs [45].

As can be seen in figure 14, when YHCFNP and carbon nanotube were mixed together, they were uniformly dispersed. In this case, CNTs can be used as the carrier and entanglement (diameter: 10 – 20 nm, length: 1–2 μm) to fix YHCFNP on the electrode surface.

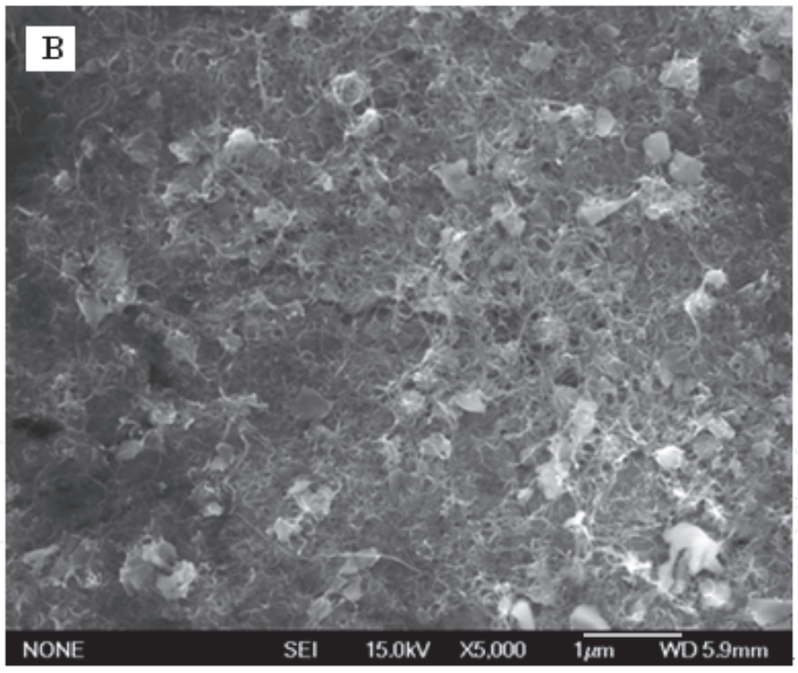

Fig. 14. Typical SEM images of the mixed YHCFNP and CNTs

Figure 15 shows the cyclic voltammograms of different electrodes with and without 0.5 mmol/L L-CySH in 0.1 mol/L PBS (pH 6.82). As figure 15A reveals, at the YHCFNP/CNTs/Nafion-modified GCE, there is a pair of well-defined redox peaks at 152 mV and 250 mV at a scan rate of 20 mV/s without L-cysteine. Under the same conditions, there was no redox peak at the CNTs/Nafion-modified GCE and bare GCE.

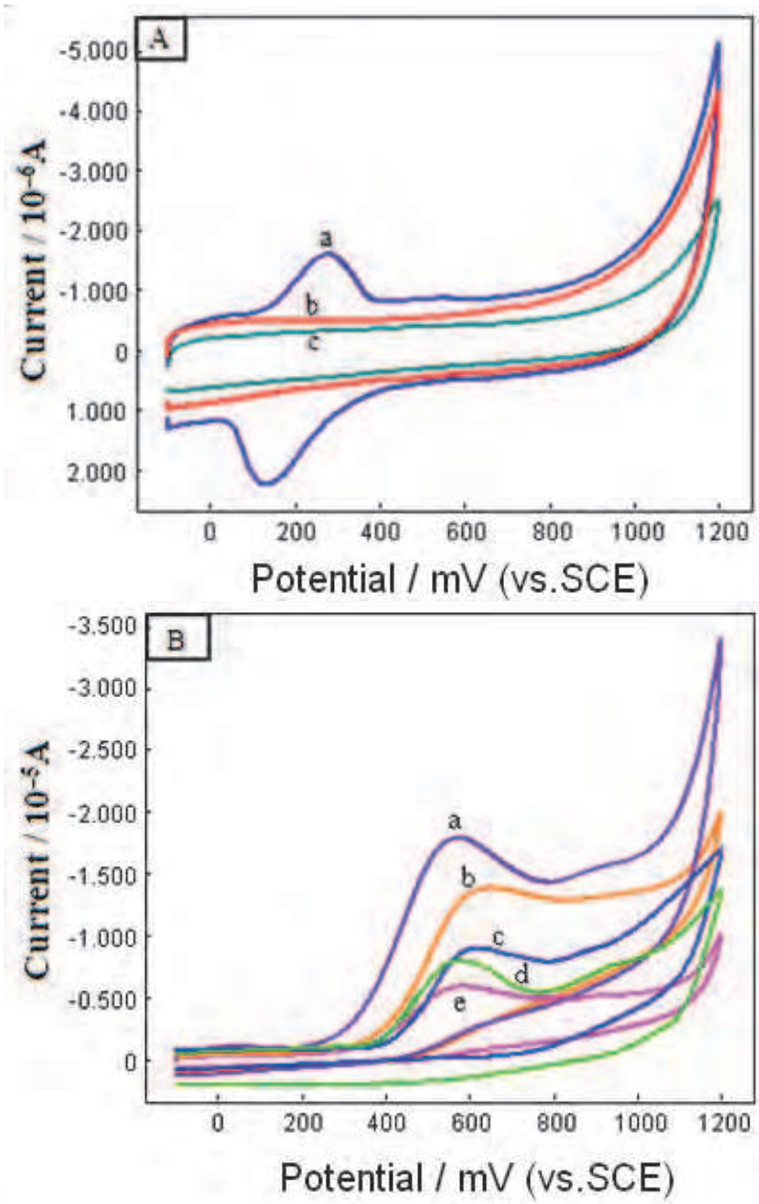

Fig. 15. A. Cyclic voltammograms of different electrodes in 0.1 mol/L PBS (pH 6.82) without L-cysteine: YHCFNP/CNTs/Nafion-modified GCE (a), CNTs/Nafion-modified GCE (b), GCE (c) ; B. Cyclic voltammograms of different electrodes in mol/L PBS (pH 6.82) with 0.5 m mol/L L-cysteine: YHCFNP/CNTs/Nafion-modified GCE (a), CNTs/Nafion-modified GCE (b), CNTs-modified GCE (c), YHCFNP-modified GCE (d), GCE (e). Scan rate 20 mV/s.

Figure 15 B depicts the cyclic voltammograms of different electrodes with the addition of 0.5 m mol/L L-CySH in 0.1 mol/L PBS (pH 6.82). L-cysteine produced a weak anodic peak at the bare GCE (c), which demonstrates the slower electrochemical reaction of L-cysteine at the GCE surface. This phenomenon may be related to electrode fouling caused by the deposition of this compound and its oxidation products on the electrode surface. At the CNTs-modified GCE (c) , there was a well-defined anodic peak , and the peak

current was clearly higher than that at the bare GCE. Indeed, in a number of cases, the L-cysteine molecules under study can interact with carbon nanotube in a way that a well-polished ''traditional'' carbon electrode cannot. This phenomenon is evidence of the catalytic effect of CNTs toward L-cysteine oxidation. In most cases, the electrocatalytic activity of carbon nanotube is attributed to edge plane like-sites/defects, which may occur at the ends, and along the tube axis [46]. Recently it has been revealed that additionally, metallic impurities remaining from the fabrication processes can be the origin for certain analytes [47–49]. Because of the excellent evenly dispersing capacity of Nafion for CNTs, a stronger anodic peak of L-CySH was shown at the CNTs/Nafion-modified GCE (b). At the YHCFNP-modified GCE (d), a well-defined anodic peak appeared. The peak current was obviously higher than that at the bare GCE, which demonstrated that the YHCFNP-modified GCE can improve the electrochemical reaction of L-cysteine on the electrode surface. In addition, a well-defined anodic peak appeared at the YHCFNP/CNTs/Nafion-modified GCE (a), and the height of the anodic peak was clearly higher than that at the CNTs/Nafion-modified GCE. The anodic potential (E_{pa}) was about 570 mV. In contrast, the anodic potential at the CNTs/Nafion-modified GCE was 642 mV, indicating a negative shift of about 72 mV. The experimental results indicate that the electrooxidation of L-CySH is remarkably improved by the YHCFNP/CNTs/Nafion-modified GCE, which may result from the high dispersion of YHCFNP/CNTs nanocomposite with high surface area and good electronic properties.

Under the optimum experimental conditions, the electrochemical response to L-cysteine at the YHCFNP/CNTs/Nafion-modified GCE was fast (within 4 s). Linear calibration plots were obtained over the range of 0.20–11.4 μmol/L with a low detection limit of 0.16 μmol/L. The YHCFNP/CNTs/Nafion-modified GCE exhibited several advantages, such as high stability and good resistance against interference by ascorbic acid and other oxidizable amino acids.

7. Concluding remarks

Nowadays, the study of CNTs modified electrode is the forefront subject that offers enormous possibilities in pharmaceutical analysis. The facility of the preparation and functionalization of CNTs makes them very useful for the development of modified electrodes with specific detection of medicine molecules, as well as for the fabrication of third generation sensors (no mediator is needed). As far as the modified electrode is concerned, the CNTs coated and polymer embedded electrodes are more widely used than the CNTs paste electrode and CNTs intercalated electrode in the determination of pharmaceutical analysis owing to the different dispersants. Thus, to explore and use the materials as dispersants with good and green friendly properties is an important field. Moreover, CNTs intermingled with other nonmaterials (such as nano Au particles, nano YHCF, *etc*) were modified on conventional electrodes. These nanocomposites provide a synergic effect which results in the improvement in the response property of modified electrodes. So, CNTs hybrid with other nanomaterials used as modified material was also an important part. In addition, further research on the mechanism of the electrochemical reaction between medicine and modified electrode is a very important aspect in relation to CNTs modified electrode. Although CNTs modified electrode used in pharmaceutical analysis is receiving increasing interest for sensor construction in recent years, the study should involve the combination of nanomaterials, analysis and life sciences.

8. References

[1] S. Iljima, Nature. 354 (1991) 56.
[2] Y.R. Wang, P. Hu, Q.L. Liang, G.A. Luo, Y.M. Wang, Chin. J. Anal. Chem. 36 (2008) 1011.
[3] D. M. Graham, Nutr. Rev. 1978, 36, 97.
[4] A. Turnball, J. Br. Nutr. Found. Nutr. Bull. 1981, 6, 153.
[5] S.L. Yang, R. Yang, G. Li, L.B. Qu, J.J. Li, L.L Yu, J. Electroanal. Chem. 639 (2010) 77.
[6] S.L. Yang, R. Yang, G. Li, J.J. Li, L.B. Qu, J. Chem. Sc. 122 (2010) 919.
[7] Y.C. Tsai, J.M. Chen , S.C. Li , F. Marken, Electrochem. Commun. 6 (2004) 917.
[8] D. Sun, Z.M. Sun, J. Appl. Electrochem. 38 (2008)1223.
[9] Y.C. Tsai, J.M. Chen, F. Marken, Microchim. Acta. 150 (2005) 269.
[10] K.B. Wu, S.S. Hu, Microchim. Acta. 144 (2004) 131.
[11] W.S. Huang, C.H. Yang, S.H. Zhang, Anal. Bioanal. Chem. 375 (2003) 703.
[12] R.X. Guo, Q.Xu, D.Y. Wang, X.Y. Hu, Microchim. Acta. 161 (2008) 265.
[13] A. Belay, K. Ture, M. Redi-Abshiro, A. Asfaw, Food. Chem. 108 (2008) 310.
[14] American Beverage Association, Nutrition & Health, Ingredients, Caffeine, http://minisites.ameribev.org/products/pdf/caffeine-levels.pdf, last accessed October, 2009.
[15] B.A. Fox, A.G. Cameron, Food Science, Nutrition and Health, 15th Ed. Edward Arnold, London. 1989.
[16] Combs GF, The Vitamins: Fundamental Aspects in Nutrition and Health, 2nd ed., Academic Press, San Diego. 1992.
[17] O.Arrigori, C.D. Tullio, Biochim. Biophys. Acta. 1569 (2002) 1
[18] J.M. Zen, J.J. Jou, G. Ilangovan, Analyst. 123 (1998) 1345
[19]G. Li, S.L. Yang, L.B. Qu, R. Yang, J.J. Li, J. Solid. State. Electrochem. 15 (2011) 161.
[20] S.H. Kim, S.A. Kim, M.K. Park, Int. Immunopharmacol. 4 (2004) 279.
[21] X.A. Wu, H.L. Chen, X.G. Chen, Biomed. Chromatogr 17 (2003) 504.
[22] P. Drasar, J. Moravcova, J. Chromatogr. A. 812 (2004) 3
[23] T.Y.K. Chan, Drug Saf. 17 (1997) 209.
[24] S.L. Yang, L.B. Qu, R. Yang, J.J. Li, L.L. Yu, J. Appl. Electrochem. 40 (2010) 1371.
[25] Y. Wang, J. Wu, D. Li, Chin. J. Anal. Chem. 34 (2006) 1331.
[26] Y.L. Chang, B. Liu, Zhongguo Zhong Yao Za Zhi. 31 (2006) 653.
[27] K. Yu, Y.W. Wang, Y.Y. Cheng, J. Pharm. Biomed. Anal. 40 (2006) 1257.
[28] R.M. Wightman, L.J. May, A.C. Michael, Anal. Chem. 60 (1988) 769A.
[29] A. Liu, I. Honma, H.S. Zhou, Biosens. Bioelectron. 21 (2005) 809.
[30] J.W. Mo, B. Ogorevc, Anal. Chem. 73 (2001) 1196.
[31] S.L. Yang, G. Li, R. Yang, M.M. Xia, L.B. Qu, J. Solid. State. Electrochem. DOI 10.1007/s10008-010-1210-x.
[32] T. Sagara, K. Niki, Langmuir. 9 (1993) 831.
[33] R.M. Gene, C. Cartana, T. Adzet, E. Marin, T. Panella, S. Canigueral, Planta. Med. 62 (1996) 232.
[34] A. Hasan, I. Ahmad, Fetoterapia. 67 (1996) 182.
[35] R. Ramanathan, W.P. Das, C.H. Tan, Int.. J. Oncol. 3 (1993) 115.
[36] W.Q. Sun, J.F. Sheng, Handbook of Natural Active Constituents, Chinese Medicinal Science and Technology Press, Beijing, 1998, 2240

[37] J.E.F. Reynolds, Martindale. The Extra Pharmacopoeia, 31 ed., The Royal Pharmaceutical Society, Council of the Royal Pharmaceutical Society of Great Britain, London, 1996, 1679.
[38] J. van der Geer, J.A.J. Hanraads, R.A. Lupton, J. Sci. Commun. 163 (2000) 51.
[39] S.L. Yang, L.B. Qu, G. Li, R. Yang, C.C. Liu, J. Electroanal. Chem. 645 (2010) 115.
[40] Dorland's Illustrated Medical Dictionary, 27th. d., E.J. Taylor, d.;W.B. Saunders: Philadelpia, 1988.
[41] D.Voet, J. G. Voet, Biochemistry, 2nd ed.; John Wiley & Sons: New York, 1995, 1263.
[42] W. Dro¨ge, H. P. Eck, S. Mihm, Immunol. Today. 13 (1992) 211.
[43] O.A. Sadik, W.H. Land, J. Wang, Electroanalysis. 15 (2003) 1149.
[44] Z.F. Chen, H.Z. Zheng, C. Lu, Y.B. Zu, Langmuir. 23 (2007) 10816.
[45] L.B. Qu, S.L. Yang, G. Li, R. Yang, J.J Li, L.L Yu, Electrochim. Acta. 56 (2011) 2934
[46] C.E. Banks, T.J. Davies, G.G. Wildgoose, R.G. Compton, Chem. Commun. 7 (2005) 829.
[47] J. Kruusma, N. Mould, K. Jurkschat, A. Crossley, C.E. Banks, Electrochem. Commun. 9 (2007) 2330.
[48] M. Merisalu, J. Kruusma, C.E. Banks, Electrochem. Commun. 12 (2010) 144.
[49] J. Kruusma, V. Sammelselg, C.E. Banks, Electrochem. Commun. 10 (2008) 1872.

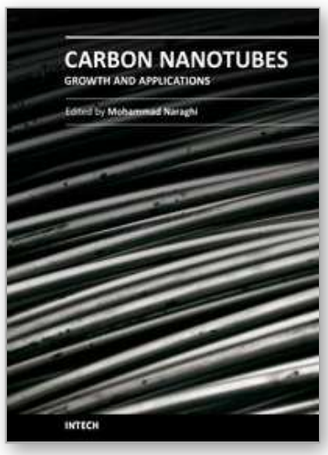

Carbon Nanotubes - Growth and Applications

Edited by Dr. Mohammad Naraghi

ISBN 978-953-307-566-2
Hard cover, 604 pages
Publisher InTech
Published online 09, August, 2011
Published in print edition August, 2011

Carbon Nanotubes are among the strongest, toughest, and most stiff materials found on earth. Moreover, they have remarkable electrical and thermal properties, which make them suitable for many applications including nanocomposites, electronics, and chemical detection devices. This book is the effort of many scientists and researchers all over the world to bring an anthology of recent developments in the field of nanotechnology and more specifically CNTs. In this book you will find:

- Recent developments in the growth of CNTs
- Methods to modify the surfaces of CNTs and decorate their surfaces for specific applications
- Applications of CNTs in biocomposites such as in orthopedic bone cement
- Application of CNTs as chemical sensors
- CNTs for fuelcells
- Health related issues when using CNTs

How to reference

In order to correctly reference this scholarly work, feel free to copy and paste the following:

Lingbo Qu and Suling Yang (2011). Application of Carbon Nanotubes Modified Electrode in Pharmaceutical Analysis, Carbon Nanotubes - Growth and Applications, Dr. Mohammad Naraghi (Ed.), ISBN: 978-953-307-566-2, InTech, Available from: http://www.intechopen.com/books/carbon-nanotubes-growth-and-applications/application-of-carbon-nanotubes-modified-electrode-in-pharmaceutical-analysis

INTECH
open science | open minds

InTech Europe
University Campus STeP Ri
Slavka Krautzeka 83/A
51000 Rijeka, Croatia
Phone: +385 (51) 770 447
Fax: +385 (51) 686 166
www.intechopen.com

InTech China
Unit 405, Office Block, Hotel Equatorial Shanghai
No.65, Yan An Road (West), Shanghai, 200040, China
中国上海市延安西路65号上海国际贵都大饭店办公楼405单元
Phone: +86-21-62489820
Fax: +86-21-62489821

IntechOpen